WWW.IJRPR.COM

International Journal of Research Publication and Reviews

Journal homepage: www.ijrpr.com ISSN 2582-7421

A Study on Welding Characteristics of Submerged Arc Welding (SAW) on Mild Steel

[1]Aijaz Hussain Mir, [2] Mukesh Kumar

[1]M. Tech Scholar, Dept. of Mech. Engineering, PKGCET PANIPAT, Haryana, India.
[2]Assistant Prof., Dept. of Mech. Engineering, PKGCET Panipat, Haryana, India
Jammalimir620@gmail.com

ABSTRACT:

SAW is fundamentally a circular segment welding process in which the curve is hidden by a cover of granular and fusible flux. Along these lines, physical properties of flux are critical contemplations in SAW for enhancing welding properties. Three parameters are taken into consideration for performing the welding these are: current(A), voltage(B) and flux(C). the range of current is 280-320 A , voltage 32-36 V and basicity index of flux 0.9-1.1-1.3.In this study we should develop three type fluxes by varying metal powder in different percentages by weight. We also study the effects of submerged arc welding process parameters on mechanical properties and weld bead and also optimize the welding parameters such as current, voltage and flux (BI).In this study we performed various tests e.g Tensile test, Impact test, Hardness test, Bead width and reinforcement test. After performing various test there is an optimum value for all welding characterstics e.g tensile strength, impact toughness, hardness, bead width and reinforcement height with the help of Taguchi technique which is performed on minitab 18. After that we perform conformation test which optimize the welding characterstics.

1. Introduction

1.1 Welding Definition

Welding is the permanent combining from two materials (usually metals) by a confined mixture formed by the proper weight, temperature, and metallurgical parameters. Numerous welding forms have been developed, ranging from high temperature along with low wt. to high wt. with low temp., depending on the combination of temperature and weight. There are numerous varieties of welding methods, such as resistance butt, metal, projection, flash, spot, and submerged arc welding. Even so, there are numerous techniques for joining metals. One of the quickest and most efficient methods is welding.

1.2 Submerged Arc Welding

SAW basically uses a circular segment welding technique. where a layer of fusible and granular flux conceals the curve. Accordingly, the physical characteristics of the flux are important considerations in SAW to improve the welding properties. The circular segment created between the workpiece and For SAW, heat comes from an exposed strong metal in the form of a reusable wire-terminal. The circular type part is maintained in the liquid flux, which protects the weld metal from barometric tainting and refines it.

1.3 Mild Steel

Mild steel is a carbon steel type with low carbon content, or "low carbon steel." The quantity of carbon, typically present into mellow steel is between 0.06% and 0.24% with weight, though ranges which depending on the source. Higher carbon steels are described as having carbon contents between 0.41% and 3.2%. If the steel contains more carbon than that, it is referred to as solid metal. Since mild steel isn't a compound steel, it doesn't contain many other elements besides iron; mellow steel doesn't have significant amounts of molybdenum, chromium, and other alloying elements. A few characteristics set it apart from higher carbon and combination steels, despite the moderately low content of alloying and carbon components. Less carbon means mild steel can be bent, machined, and welded more easily than other steels.

2. Literature Reviews

Soo Bang Kook et al, 2008, reasoned that, metal cored wires and fluxes with difference pieces were used to perform submerged circular segment welding [10]. It was investigated and determined how the wire/flux mix affected the amount of component exchange among the slag and weld metal, as well as the compound arrangement, and impact on the welded metal's strength. In many blends, the amounts of carbon and manganese show a negative value when components are transferred from the weld metal to the slag during welding. Still, the exchange measure is distinct based on the flux organization. More positive C and Mn are produced by increasingly fundamental fluxes through a decrease in the O2 content of the weld metal and an apparent increase in Mn action in the slag, respectively. On the other hand, the flux's Al2O3, TiO2, and ZrO2 components affect the exchange of silicon. Si becomes more positive as the oxides substance increases, reaching a positive estimation of 0.054. This is because there's a chance that Si will be replaced by Al, Ti, or Zr in the SiO2 configuration, which will increase the amount of Si that transfers from the slag to the weld metal. The purpose of entangled flux is to be utilized in the sharp flux mixture during the SAW procedure. In this way, the work tries to apply the concept of "waste to riches."In addition to process optimization, efforts have been made to develop scientific models that represent various parameters of the globule geometry as process factors. Consequently, research has been conducted on the four dimensions that influence the process parameters of flux basicity, slag-blend rate, and welding current. Using four complete factorial structures, we have welded mellow steel plates to produce dab on plate welds without replication. After estimating the dot width and support, we computed additional critical globule geometry parameters, like rate weakening.

Serdar Karaoglu et al. 2008, Parameters have a major impact at the makeup of a welded. Control systems and parameter advancement can benefit from the use of scientific displaying [11]. This study emphasizes the examine-ability of the parameters and varying the requirements of the parameters for the optimal weld dot geometry, instead of emphasizing the noteworthy effects of the primary process parameters. Process variables like welding voltage, current, and speed are known as structure factors. The target work is framed by the weld dab's width, stature, and entrance. The trial portion of the study is determined by three dimensional factorial plans of three process parameters. Yield parameters are impacted in relation to the information parameters following the completion of an affectability study conducted in controlled experimental settings. The effects of these three structural parameters on the dab stature and globule width show how crucial it is for these parameters to vary, even slightly, in order to affect the kind of welding activity. The results also show how virtually unaffected by variations in voltage and speed the infiltration is. After receiving Taguchi's L9 (3**3) symmetrical exhibit configuration, tests were conducted using three different dimensions of standard process parameters using welding current and flux basicity files to achieve a dot on plate weld on mild steel plate, as needed. Every trial run has included an estimation of the basic components of the dab geometry and HAZ, including the globule width, support, entrance profundity, and HAZ width. Slag produced during welding is used up by combining it with freshly applied, unmelted flux in subsequent procedures.

Saurav Datta et al, 2009, the submerged curve welding advancement issue. The aim was to examine the optimal procedure condition that would be suitable for generating the weldment's intended dot geometry parameters [13]. For the analysis, four corresponding globule geometry highlights—rate weakening, dot width, support, and profundity of infiltration—have been chosen. The approved procedure condition accounts for various variables, including voltage, wire feed rate, and navigate speed. Thousands of relevant answers have been turned into high-quality, free recordings called significant segments. Principal component analysis, or PCA, has been altered to hide various enhancement problem goals under a single goal task. The goal of this single-target project was to be a comprehensive, important component. Using Taguchi's powerful streamlining technique, the ideal configuration that can raise the composite vital segment has been linked. A satisfactory result was obtained from a corroborated test.

Vinod Kumar et al., 2009, 10% or so of all-out welding is added by submerged circular segment welding. Due to handling and transportation, between 10% and 16% of the flux is converted during welding into tiny particles known as flux dust [14]. Surface porosity may result from the inability of the gases produced during the welding process to escape, if the improbable but unlikely possibility of welding without removing these tiny particles from the flux comes to pass. Nevertheless, if sieving is necessary to remove these tiny particles, the cost of welding will increase significantly. This flux dust can also become contaminated if thrown or dumped. The range of compound synthesis and mechanical properties of each weld metal arranged from the generated fluxes and the parent fluxes were similar, according to the analysis of this study. This method allows for the generated fluxes to be arranged from the waste flux residue without sacrificing the mechanical properties of the welded joints.

Alam, Shahnwaz, et al,2011, An investigation design that uses the 2-level full factorial method has been used to direct experiments and create links between numerical models for predicting the weld dot infiltration in single wire submerged bend welding of mild steel plates that are 12 mm thick [14]. We have examined and analyzed the reaction factor, specifically the dot entrance, and how it is influenced by the following factors: wire feed rate, welding speed, circular segment voltage, current, and spout to-plate remove. The t-test, F-test, and examination of change were used, in that order, to assess the hugeness and sufficiency of the developed models. Additionally, a graphic representation of the procedure factors' individual and combined effects on the weld dab infiltration has been provided. The developed models could be used to control the weld globule quality and predict the critical weld dot entrance by choosing the right procedure parameter values.

Sudhakaran, et al., 2011, Meeting quality standards, such as dot geometry, which is greatly impacted by a number of process parameters, can result in the production of high-quality welds [15]. The welded structure will be even less satisfactory if the weld globule measurements are off. This paper reports on research on the use of genetic algorithms (GA) to advance process parameters for the advancement of profundity to width. Research was conducted using the focal composite. The critical controllable welding process parameters were correlated with the weld dab parameters (dot width, profundity to width proportion, and profundity of entrance) using a table plan and scientific models. These models were used to study the direct and indirect effects of the procedure parameters on the geometry of the weld dot. With infiltration and dot width as requirements, a Turbo C source code was created to accomplish the advancement for profundity to width proportion after the process parameters were fully optimized using GA. indicating the model's

accuracy and usability as well as the program's development. The results obtained facilitate a prompt selection of the process parameters to achieve the desired quality.

Kumar Vinod, 2011, In order to automate a welding process, which is currently the norm in the manufacturing sector scientific models linking the process parameters to the weld globule parameters must be created [16]. High dependability, deep penetration, seamless completion, and great profitability are characteristics of submerged circular segment welding (SAW), which is especially useful for welding boiler joints and funnels. Using generated fluxes, numerical models for SAW have been generated in the current work. It has been possible to predict fundamental aspects of the weld dot geometry and form connections by applying reaction surface philosophy. The ampleness and noteworthiness of the models have been evaluated separately using the F-test and the t-test. A graphical frame that illustrates the fundamental and cooperative effects of the procedure factors on the dab geometry and shape factors can be used to predict critical weld dot measurements and shape relationships, as well as control the weld globule quality by choosing the right procedure parameter values.

Saluja et al, 2012, Rati asserts that mechanical welding frameworks could be used profitably once the optimal process parameters are identified for achieving the necessary quality and the relative effects of information parameters on yield parameters are established [18]. Using the Reaction Surface Strategy method, the conditions and logical relationship between the evident mean reactions and the control factors influencing the reaction are characterized. This article develops a numerical model for the butt joint weld fortification, dot entrance, and globule width sound quality. After that, it oversees the application of the Factorial plan technique to streamline the welding current and bend voltage of the four submerged curve welding parameters.

Bamankar, Pranesh B., 2013, To investigate the effects of submerged curve process parameters, on infiltration profundity, tests are conducted on mild steel with a thickness of 12 mm. The parameters tested are welding current, circular segment voltage, and welding speed (Trolley speed) [18]. The examinations are designed with the Taguchi technique (using the Taguchi L9 symmetrical exhibit) with an emphasis on three dimensions and three components. The loader auto weld major with 900 (S) Power source manufactured by India was the focus of the investigation. As the base metal, mild steel plates with dimensions of 50 mm in length, 50 mm in width, and 12 mm in stature were used.

Filler wire made of EH 14 copper covered anode with a 2.4 mm diameter was used. Agglomerated transition using Amazon Web Services (AWS) 5.17 and Flux 10.81 (L) manufactured by ESAB Coding was used. In order to join the plates in a level position with the anode facing the plates, Transverse to the welding bearing, samples with a width of 10 mm were cut from each welded plate. These samples underwent a 10% nital (i.e., 90% liquor + 10% nitric acid) cleaning, grinding, and scratching procedure. We monitored the weld dot profiles using an optical magnifier set to 20X magnification. The dab width and the depth of infiltration were estimated. An increase in welding current deepens the aperture. It is determined that liquid metal beads are definitely overheated when they exchange from the anode to the plate. It makes perfect sense to assume that the extra warmth contributes to the work piece liquefying even more. More heat is transferred to the base plate as a result of the beads' expanding warmth substance and rising temperature as a result of increased current. As the current increases, the beads' size decreases but their energy increases, creating a deeper entrance or space when they strike the weld pool. Improved heat input and power curves per unit length of the welded dot led to higher current thickness, which in turn softened a high volume of the base-metal and allowed for deeper entrance, which could also account for the increase in infiltration as current increased.

Suck-Joo Na and Venkata Kiran Degala, 2014, At an iso-heat contribution of 3.5 kJ/mm, the effect of the main and trailing circular segment welding current on the quality of the two-wire pair submerged (SAW-T) bend weld was observed [19]. Weld dab measurements, the amount of time the weld pool cools down from 700 to 500 °C, the weld dot ferrite stage portion, and smaller scale hardness are all included in the weld quality. Based on the temperature circulation predicted by the numerical model, the cooling time was calculated.

The weld entrance essentially decreased with decreasing driving circular segment current at a low dimension of trailing curve current for a consistent warmth input, whereas the final weld infiltration was less sensitive to the main bend current at higher trailing bend current. When driving bend current was increased from 800 to 1000 An with a constant trailing circular segment current and warmth contribution of 1050 An and 3.5 kJ/mm Whatever the case, lower flows were associated with shorter weld pool cooling times. In the current study, welds supplied at a welding rate of 27.80 mm/s and a main and trailing bend current of 1050 An resulted in higher-quality, highly efficient weld globules. The weld pool acicular ferrite stage volume part increased slightly and the allotriomorphic ferrite stage measurement decreased when the main or trailing circular segment current was increased at a constant warmth input.

Prachya Peasura, 2017 At an iso-heat contribution of 3.5 kJ/mm, the effect of the main and trailing circular segment welding current on the two-wire couple submerged curve weld quality was discovered [20]. Weld dot measurements, miniaturized scale hardness, weld dot ferrite stage division, and cooling time in the weld pool from 800 to 600 °C are all included in the weld quality. The temperature circulation that the numerical model predicted was used to calculate the cooling time. Weld infiltration dramatically reduced at a low dimension of trailing circular segment current with diminishing driving curve current for a constant warmth input. At higher trailing bend current, the final weld entrance was less susceptible to the main bend current. When driving circular segment current was increased from 800 to 1000 An while maintaining a constant trailing bend current and a warmth contribution of 1050 An and 2.5 kJ/mm, there was no discernible critical variation in the typical weld pool time from 700 to 600 °C. However, at higher flows, the shortest weld pool cooling time was observed. The weld pool acicular ferrite stage volume portion increased slightly and the allotriomorphic ferrite stage measurement decreased when the main or trailing curve current was increased at a constant warmth input. This also caused the weld globule smaller scale hardness to slightly increase. In the current investigation, welds produced at a welding velocity of 26.80 mm/s and a main and trailing circular segment current of 1050 An showed higher quality and high efficiency weld dabs.

Ajitanshu Vedrtnam, 2018, For the welding, a consistent voltage fully programmed SAW machine with a 3.2 mm treated steel anode, 700A, 3-stage, 60 Hz rectifier type control source was used [21]. Using a 4.2 mm wire reel, weld globules were kept in storage in accordance with the hardened steel tests' structural framework of 101.6 × 76.2 × 10 mm3. Before the examples were physically attached to the welding bed with the necessary earth association, they were cleaned with a brush to remove any residue and rust. To remove any slag, the welded tests were cleaned. The measurements of dot width and dab stature are made with a vernier caliper. Every exploratory run (using the same information sources) was carried out several times, and in order to reduce error, the standard dab width and height were regarded as definitive readings. Using a Rockwell hardness analyzer, hardness was calculated. Using RSW, relapse investigation, and GA, In the SAW, the ideal weld dab width, dab stature, and dot hardness were found by determining the procedure parameters. It was discovered that the overall weld parameters have an impact on the reaction factors chosen for the investigation. The findings indicate that while an increase in current causes an increase in globule height but no change in dot width, an increase in voltage causes an increase in dot width but a decrease in dot height. The globule width and stature decrease with increased welding speed. The dab width decreases and the globule height increases as the spout to-plate separation increases. Voltage and travel speed have little effect on the dab hardness, which rises with current. Both the trial results under comparison and the expectations from the scientific model developed by RSM are reasonably understood. When compared to the relations derived from the relapse investigation, as confirmed by the confirmation tests. The relapse analysis and buildup plots show that error is contained within striking breaking points.

3. Design of Experiment (DOE)

Increasing productivity and improving quality are essential goals for any company. The methods for determining how to increase quality and profitability are developing. They have evolved from costly and time-consuming exploratory expeditions to the innovative, exquisite, and astutely profitable factual methods. When there is diversity available, the Design of Experiments (DOE) serves as the framework for all data collection procedures.

irrespective of whether the experimenter has complete control over it or not. Nevertheless, these terms are typically used in measurements for controlled research. The articles on hypothesis surveys, measurable studies, characteristic analyses, and semi tests (such as semi test plans) discuss various types of studies and their structures.

3.1 Taguchi Method

The Taguchi system is an eminent methodology that gives a precise and powerful strategy for procedure upgrade. It has been comprehensively used for thing structure and procedure streamlining far and wide. This is a direct result of the advantages of the structure of test using Taguchi's technique, which joins improvements of exploratory course of action and probability of examination of association between different parameters. Lesser number of examinations is required in this procedure. As a result, time similarly as cost is decreased fundamentally. Taguchi proposes test plan similarly as symmetrical group that gives assorted mixes of parameters and their measurements for every examination. According to this strategy, the complete parameter space is analyzed by unimportant no. of indispensable examinations in a manner of speaking. In perspective on the typical yield estimation of the quality trademark at each level, essential effect examination is performed. The determination of which process parameter is truly fundamental and the allocation of each strategy parameter to the yield trademark are then determined by examining change analysis of variance. With the rule effect and ANOVA examinations, possible mix of perfect parameters can be foreseen.

5.1 Tensile Test Readings

Tensile tests have been conducted with a universal tensile testing apparatus. 125.5 KN is the ultimate tensile load on the base metal. Using IS 3613-1974 as a guide, which includes the acknowledgment test specifications Table 5.1 displays the elongation and stress values. The UTM is then used to take readings for a variety of joints made with different kinds of flux.

Table 5.1: Ultimate Tensile Stress Readings according to IS 3613-1974

Maximum Tensile Stress	Elongations
More than 350 N/mm^2	More than 22%

Table 5.2: Maximum values for Tensile Load

Flux	Index of Basicity	Maximum Values for Tensile Load(KN)
1	0.7	104.56
2	2.3	121.64
3	2.5	113

Table 5.3: Maximum Tensile Stress Values

Flux	Index of Basicity	Avg Max. Tensile Stress (N/mm^2)	Avg Displacement (mm)	Avg Percentage Elongation
1	0.9	329	9.7	19.4
2	1.1	408	13.2	27.38
3	1.3	393	12.8	25.6

Every specimen examined falls within IS 3613-1974's parameters. Thus, every wire-flux combination is allowed, with the exception of flux1, which is likewise close to the BIS values. The mechanical behaviour of the parent metal change through the welding process as a result of changes to its elemental components, and the filler electrode modifies the base metal's microstructure. We looked at how different fluxes affected the welded joints' ultimate tensile stress and load. Based on Table 5.2, it can be inferred that Specimen No. 2 had the highest ultimate tensile load of 120.65 KN, while Specimen No. 1 had the lowest ultimate tensile load of 103.55 KN. According to Table 5.3, specimen number two appears to have the highest ultimate tensile stress, measuring 408 N/mm2, while specimen number one appears to have the lowest ultimate tensile load, measuring 329 N/mm2. Thus, it is evident that flux 2 is utilized in situations where high tensile strength is required.

5.2 Impact Test

The resulting weld joints' durability was assessed using the Charpy test (J). Figure 5.1 displays specimens following a room-temperature impact toughness test. Base metal has an impact toughness of 90 joules.

Fig. 5.1: Impact testing Samples

Table 5.4: Toughness Readings according to IS 3613-1974

S. No.	**Property**	**Reading according to IS 3613-1974**
1	Toughness	More than 35 J

Table 5.5 : Toughness Values

S. No.	**Basicity Index**	**Impact toughness (Joule)**	**Average toughness (Joule)**
1	0.9	88+90+84	87.3
2	1.1	100+104+98	100.6
3	1.3	85+80+76	80.3

The impact toughness values of the room-temperature weld-metals are report in Table 5.5 along with the outcomes of the impact tests that were performed on each specimen. Every specimen examined falls within IS 3613-1974's parameters. Therefore, any wire-flux combination is allowed. The Charpy impact toughness increases as tensile strength increases, as Table 5.5 makes evident. The impact toughness of the welds is influenced by a number of variables, such as the microstructure, percentage of different flux constituents, and hardness level. With the exception of flux 2, the average impact value across all specimens is below than the base-metal values.

5.3 Hardness

The hardness were taken in the weld pool and base metal. Each bead was given three readings, and the analysis relied on the average of the readings. It displays the parameter or factor with the greatest sway. Using a 95% confidence interval, the analysis has been conducted. In this study, the three dependent variables that are being examined are hardness, bead width, and reinforcement. The table below displays the observed results for each parameter. The hardness, bead width, and reinforcement values for the nine trials with three replications are listed in the table. The F ratio value should be greater than the value indicated in the F-ratio Table, according to the significance value principle. The F test's guiding principle states that a large F value in relation to an e-pooled sample indicates a significant factor. We now analyze the developed matrix in more detail.

5.4 ANOVA Method for Hardness Measurement

The degree of variety that is present as a reaction makes it easy to identify the control factors that could result in less variety (better quality). The width, hardness, and deeper entrance of the weld bead geometries, the hardness of the weld dots, all conform to the higher-the-better quality trademark. The following formula can be used to express the greater the better quality trademark's loss capacity:

$$\frac{S}{N_{(Bigger)}} = -10 \log\left(\frac{\Sigma\left(1/y_i^2\right)}{n}\right)$$

Qualitative characteristics are thus obtained in relation to the weld dab geometry's globule width and hardness. Table 5.6 displays the S/N ratio that corresponds to each level.

Table 5.6 Hardness Values by ANOVA

S. No	Currents	Voltages	Flux	Hardness (HRB)			S/N Ratio (Larger the better)	S/N Ratio (Mean)
				Response 1	Response 2	Response 3		
1	280	32	1	85	87	88	-19.4448	38.5883
2	280	34	2	91	91	94	-19.7313	39.1808
3	280	36	3	107	109	108	-20.3342	40.5876
4	300	32	2	91	92	93	-19.6848	39.1808
5	300	34	3	109	107	108	-20.3342	40.7485
6	300	36	1	101	100	99	-19.9564	40.0864
7	320	32	3	110	114	112	-20.4922	40.8278
8	320	34	1	102	101	99	-19.9564	40.172
9	320	36	2	106	107	101	-20.0432	40.5061

Table 5.6 makes it evident that the maximum hardness (HRB) for flux 3 was measured in the welded region. This is because the weld metal's hardness value fluctuates in tandem with the carbide contents, which are present in the flux due to CrC. Oxidation processes that occurred during welding operations are typically to blame for the increase in hardness at the welding interface. The fundamental idea behind the F-test is that the more significant the impact of a procedure parameter adjustment on the execution trademark, the higher the F esteem for that parameter. The ANOVA Table shows that voltage (F 21.08 value), flux (F 79.88 value), and current (F 37.69 value) are the variables that significantly affect hardness. The main factor affecting hardness is flux. Table 5.7 shows that current, voltage, and flux have significant values.

Table 5.7: Hardness (S/N ratio)

Source	**SS**	**DOF**	**V**	**%contribution**	**F-Ratio**
Current	1.24554	2	0.622773	26.98922	37.69252*
Voltage	0.69662	2	0.348314	15.09496	21.08127*

Flux	2.63975	2	1.319879	57.19978	79.88389*
Travel speed	-	-	-	-	-
Error	0.03304	2	0.016522	0.716037	-
T	4.61497	8	-	100	-
Significant at 95 % confidence level			$F_{critical}$=19		
SS=Sum of Squares	DOF=Degree of Freedom		V:=Variance		

F ratios higher than the F ratio The parameters are significant, as indicated by the table values. In terms of increasing hardness, flux has the largest contribution (57%) and is followed by voltage (15%) and current (27%).

Table 5.8 for hardness (Raw data)

Source	**SS**	**DOF**	**V**	**%contribution**	**F-Ratio**
Current	472.888889	2	236.4444	25.6077	74.40559*
Voltage	242.666667	2	121.3333	13.14079	38.18182*
Flux	1067.55556	2	533.7778	57.80987	167.972*
Travel speed	-	-	-	-	-
Error	63.5555556	20	3.177778	3.441637	-
T	1846.66667	26	-	100	-
Significants at 95 % confidence level			$F_{critical}$ =3.4928		
SS= Sum of Squares	Deegre of fridom=Degree of Freedom		V=Variance		

Current, voltage, and flux have significant values, as Table 5.8 demonstrates. F ratios higher than the F ratio The parameters are significant, as indicated by the table values. The largest contributor to increasing hardness (57%) was flux, followed by voltage (13%), current (25%) and other factors.

5.4.1 Current's Impact on Hardness

Hardness of the welded metal was found to be influenced by welding current; hardness increased with a 280 to 320 A increase in welding current, from 96 HRB to 106 HRB.

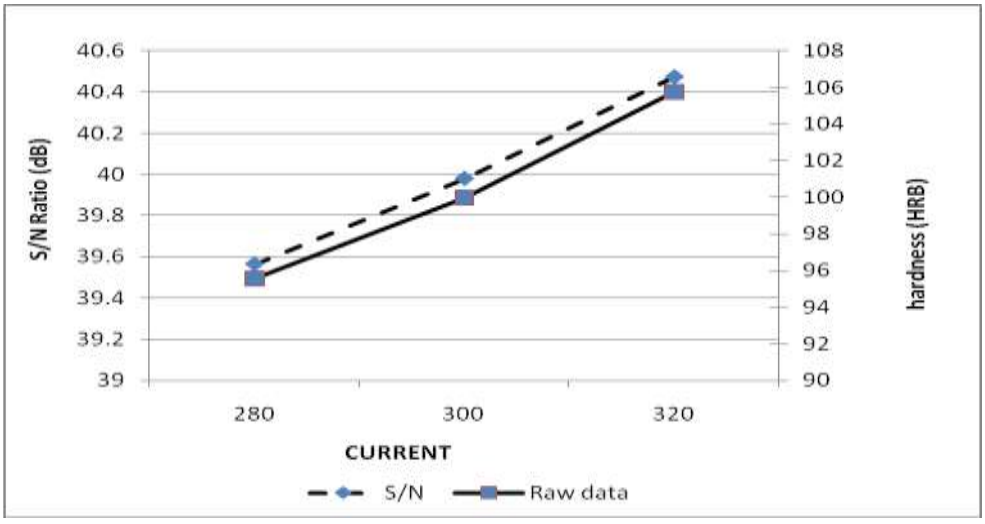

Fig. 5.2 Current Impact on Hardness

5.4.2 Voltage Impact on Hardness

Hardness has been shown to rise with increasing welding voltage. The primary cause of the hardness increase is the flux ingredients. Hardness is, however, influenced by process parameters, primarily as a result of chemical reactions that take place during welding.

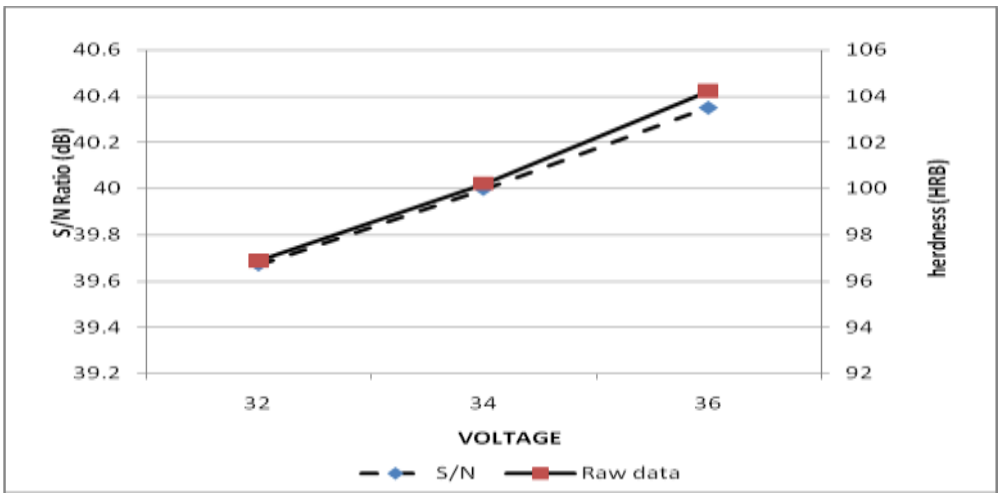

Fig. 5.3 Voltage Impact on Hardness

5.4.3 Flux Impact on Hardness

The composition of the wire and flux is important in forming the weld microstructure and achieving the desired properties in the weldment. In fluxes containing TiO, acicular ferrite enhances the mechanical characteristics of the welds. Hardness rises with increasing titanium content, improving mechanical properties. As the B.I. of flux increases, so does hardness.

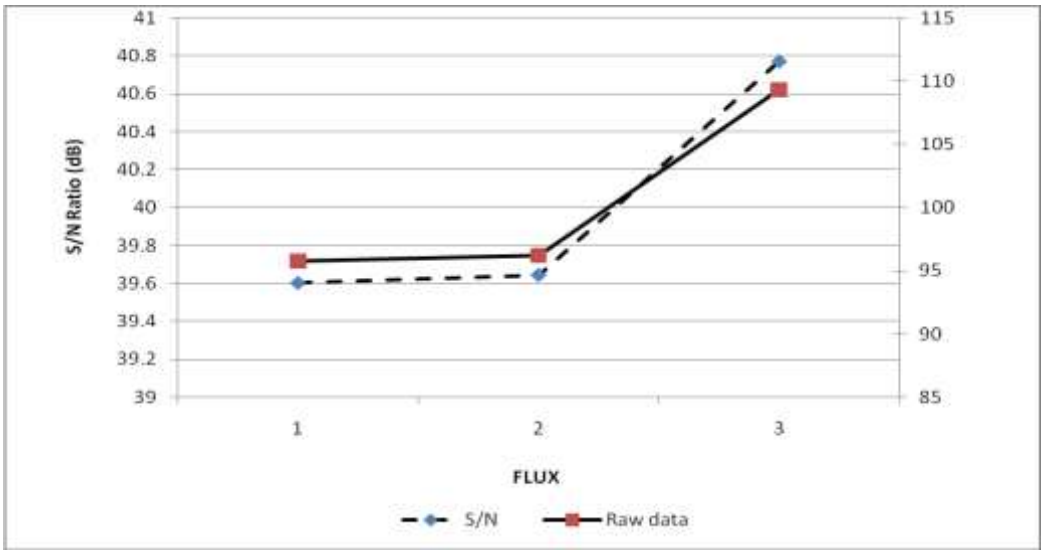

Fig. 5.4 Flux Impact on Hardness

A 7 mm thick plate by an arc voltage of 36 V, flux of 3, and welding current of 320 A yields the optimal hardness. These numbers come from Figs. 5.2, 5.3, and 5.4.

6.1 Conclusions

- To determine the optimal process parameters and their impacts in the current study. The findings led to the following deductions: The tested specimens fall within IS 3613-1974's parameters. Therefore, all wire-flux combinations aside from flux 1 are allowed.
- The submerged arc welded mild steel joint with Flux 2 and BI 1.1 had the highest tensile strength and stress.
- As tensile strength rises, so does impact strength. The highest toughness of a joint created by flux 2 welding is 100 joules.
- With the exception of joints created using flux 2, all joints have an impact strength lower than base metal.

- The ideal process parameters for maximizing the hardness of a submerged arc welded mild steel joint are flux 3, voltage of 36 volts, and current of 320 A.
- As current, voltage, and flux B.I. increase, so does the level of difficulty.
- Since hardness plays a significant role in current, the ideal voltage and maximum hardness value should be achieved.

References:

1). Vinod Kumar,Modeling of Weld Bead Geometry and Shape Relationships in Submerged Arc Welding using Developed Fluxes, 2011.

2). Rati Saluja & K M Moeed, Modeling and Parametric Optimization using Factorial Design Approach of Submerged Arc Bead Geometry for Butt Joint, 2012.

3). Pranesh B. Bamankar, Dr. S.M. Sawant, "Study of effect of process parameters on depth of penenetration and bead width in saw process",International Journal of Advanced Engineering research and studies E-ISSN2249-8974 IJAERS/Vol.II/Issue III/aprail-june 2013.

4). Degala Venkata Kiran and Suck-Joo Na. Experimental Studies on Submerged Arc Welding Process. Journal of Welding and Joining(Vol. 32, No. 3) 2014.

5). Prachya Peasura "Investigation of the Effects of Submerged Arc Welding Process Parameters on the Mechanical Properties of Pressure Vessel Steel ASTM A283 Grade A" Journal of engineering vol.7, article ID 9048324,8 pages

6). Ajitanshu Vedratnam, Gyanendra singh "Optimizing submerged arc welding using response surface methodology , regression analysis , and genetic algorithm. Elsevier 2018

7). Byrne D.M. and Taguchi G. "The Taguchi approach to parameter design", Quality Progress, Vol. 20(12), pp. 19-26, 1987.

8). Fuzzy Logic Optimization of Weld Properties for SAW using Silica Based Agglomerated Flux, Procedia Comput. Sci. (2015).

9). Optimization of vickers hardness and impact strength of silica based fluxes for submerged arc welding by Taguchi method Mater. Today:. Proc. (2015).

10). Optimization of Process Parameters of Submerged Arc Welding by Taguchi Method, Materials Today: Proceedings (2020).

11). Microstructural and mechanical evaluations of SAW by manufactured granular basic bonded Cr, Mo, and Cr–Mo active fluxes on ST37 low carbon steel, International Journal of Advanced Manufacturing Technology, (2022).

12). Tiwan; Ilman, M.N.; Kusmono; Sehono. Microstructure and Mechanical Performance of Dissimilar Friction Stir Spot Welded AA2024-O/AA6061-T6 Sheets: Effects of Tool Rotation Speed and Pin Geometry. Int. J. Lightweight Mater. Manuf. 2023, 6, 1–14.

13). Mehta, K.P.; Badheka, V.J. Effects of Tool Pin Design on Formation of Defects in Dissimilar Friction Stir Welding. Procedia Technol. 2016, 23, 513–518.

14). Palani, K.; Elanchezhian, C.; Vijaya Ramnath, B.; Bhaskar, G.B.; Naveen, E. Effect of Pin Profile and Rotational Speed on Microstructure and Tensile Strength of Dissimilar AA8011, AA01-T6 Friction Stir Welded Aluminum Alloys. Mater. Today Proc. 2018, 5, 24515–24524.

15). Raturi, M.; Garg, A.; Bhattacharya, A. Joint Strength and Failure Studies of Dissimilar AA6061-AA7075 Friction Stir Welds: Effects of Tool Pin, Process Parameters and Preheating. Eng. Fail. Anal. 2019, 96, 570–588.

16). Raturi, M.; Bhattacharya, A. Appraising Tool Wear during Secondary Heating Assisted Dissimilar Friction Stir Welding between 6061 and 7075 Aluminium Alloys. Mater. Trans. 2023, 64, 485–491.

17). Mehta, M.; Reddy, G.M.; Rao, A.V.; De, A. Numerical Modeling of Friction Stir Welding Using the Tools with Polygonal Pins. Def. Technol. 2015, 11, 229–236.

18). Yuvaraj, K.P.; Ashoka Varthanan, P.; Haribabu, L.; Madhubalan, R.; Boopathiraja, K.P. Optimization of FSW Tool Parameters for Joining Dissimilar AA7075-T651 and AA6061 Aluminium Alloys Using Taguchi Technique. Mater. Today Proc. 2021, 45, 919–925.

19). Krishna, M.; Udaiyakumar, K.C.; Mohan Kumar, D.K.; Mohammed Ali, H. Analysis on Effect of Using Different Tool Pin Profile and Mechanical Properties by Friction Stir Welding on Dissimilar Aluminium Alloys Al6061 and Al7075. IOP Conf. Ser. Mater. Sci. Eng. 2018, 402, 012099.

20). El-Hafez, H.A.; El-Megharbel, A. Friction Stir Welding of Dissimilar Aluminum Alloys. World J. Eng. Technol. 2018, 6, 408–419.

21). Abd El-Hafez, H. Mechanical Properties and Welding Power of Friction Stirred AA2024-T35 Joints. J. Mater. Eng. Perform. 2011, 20, 839–845.

22). Kumar, N.; Monga, I.; Kumar, M. An Experimental Investigation to Find out the Effect of Different Pin Profile Tools on AA 6061 T6 and AA 2014 T4 with Friction Stir Welding. Int. J. Technol. Res. Eng. 2015, 2, 1622–1625.

23). Battina, N.M.; Vanthala, V.S.P.; Chirala, H.K. Influence of Tool Pin Profile on Mechanical and Metallurgical Behavior of Friction Stir Welded AA6061-T6 and AA2017-T6 Tailored Blanks. Eng. Res. Express 2021, 3, 035026.

24). Jayaprakash, S.; Siva Chandran, S.; Sathish, T.; Gugulothu, B.; Ramesh, R.; Sudhakar, M.; Subbiah, R. Effect of Tool Profile Influence in Dissimilar Friction Stir Welding of Aluminium Alloys (AA5083 and AA7068). Adv. Mater. Sci. Eng. 2021, 2021, 7387296.

25). Meyghani, B.; Awang, M. The Influence of the Tool Tilt Angle on the Heat Generation and the Material Behavior in Friction Stir Welding (FSW). Metals 2022, 12, 1837.

26). Dialami, N.; Cervera, M.; Chiumenti, M. Effect of the Tool Tilt Angle on the Heat Generation and the Material Flow in Friction Stir Welding. Metals 2018, 9, 28.

27). Khan, N.Z.; Siddiquee, A.N.; Khan, Z.A.; Shihab, S.K. Investigations on Tunneling and Kissing Bond Defects in FSW Joints for Dissimilar Aluminum Alloys. J. Alloys Compd. 2015, 648, 360–367.

28). Di Bella, G.; Alderucci, T.; Favaloro, F.; Borsellino, C. Effect of Tool Tilt Angle on Mechanical Resistance of AA6082/AA5083 Friction Stir Welded Joints for Marine Applications. In Proceedings of the 16th CIRP Conference on Intelligent Computation in Manufacturing Engineering, CIRP ICME ’22, Naples, Italy, 13–15 July 2022.

29). Kunnathur Periyasamy, Y.; Perumal, A.V.; Kunnathur Periyasamy, B. Influence of Tool Shoulder Concave Angle and Pin Profile on Mechanical Properties and Microstructural Behaviour of Friction Stir Welded AA7075-T651 and AA6061 Dissimilar Joint. Trans. Indian Inst. Met. 2019, 72, 1087–1109.

30). Fuller, C.B. Friction Stir Tooling: Tool Materials and Designs. In Friction Stir Welding and Processing; Mishra, R.S., Mahoney, M.W., Eds.; Springer: Cham, Switzerland, 2007. 118. Mishra, R.S.; Ma, Z.Y. Friction Stir Welding and Processing. Mater. Sci. Eng. R Rep. 2005, 50, 1–78.